Accelerated in vitro degradation properties of polylactic acid/phosphate glass fibre composites

Reda M. Felfel[1,2] · Kazi M. Zakir Hossain[1] · Andrew J. Parsons[1] ·
Chris D. Rudd[1] · Ifty Ahmed[1]

Abstract Degradation properties were studied for polylactic acid (PLA) and phosphate glass fibre ($40P_2O_5$–$24MgO$–$16CaO$–$16Na_2O$–$4Fe_2O_3$, denoted as P40) reinforced unidirectional (UD) and randomly mat (RM) PLA composites using phosphate buffer saline (PBS) media over a range of temperatures from 21 to 85 °C. Glass transition and melting temperatures for PLA decreased from 61.3 and 167.4 to 52.7 and 151.6 °C, respectively, and crystallinity increased from 9.2 to 58.3 % during 3 days of degradation period in PBS media at 85 °C. Appearance of sharp crystalline peaks after degradation at higher temperatures which was confirmed via X-ray diffraction analysis was also indicative of increase in crystallinity. However, flexural strength decreased by approximately 20 % (for PLA) and by around 50 % (P40 RM and P40 UD composites) of the initial strength after degradation in PBS at 37 °C. No significant changes in mechanical properties were observed before and after degradation of composites at 21 °C for 56 days. Monomodal molecular weight distribution for the PLA before and after degradation in PBS at 37 °C was replaced by bimodal after degradation at higher temperatures. Arrhenius equation applied for the change in molecular weight of the polymer and composite samples and the obtained degradation activation energies were 85.4, 78.7 and 74.1 kJ mol^{-1} for PLA within PLA alone, P40 RM and P40 UD composites, respectively. Time prediction was applied to correlate short-term degradation (at elevated temperatures) to the long-term effects (at 37 °C) using both 'tipping point' and molecular weight as co-ordinates.

Introduction

The degradation behaviour of bioresorbable polymers and composites plays a crucial role in the choice of material for bone fixation applications. Many factors affect the degradation rate of the polymers such as chemical structure, crystallinity, molecular weight and molecular weight distribution, temperature, and pH. The effect of temperature is particularly remarkable to access the accelerated degradation properties [1–4]. The influence of temperature on the degradation process is not only useful in understanding the resorption behaviour of the devices in vivo, but also it is important for developing a model to predict the life time of the device using an accelerated degradation method. Some polymers take more than 3 years for complete degradation, such as poly-L-lactic acid (PLLA) [5], which depends on the environment as well as the molecular weight of polymer. This has prompted the use of different methods in order to shorten the time of degradation studies, but it is difficult to guarantee that the results will remain valid at body temperature (37 °C) [2]. However, with appropriate precautions, degradation studies conducted at higher temperatures can be of great value and result in saving time and research funds [6].

Temperature has a crucial effect on the degradation of absorbable polymers. Firstly, the rate of hydrolysis increases with degradation temperature, potentially making possible a correlation between short-term effects at high temperature and long-term effects at physiological temperature. Secondly, body temperature varies between the human and certain animals such as rabbits and pigs that are used as *in vivo* models [2].

✉ Reda M. Felfel
reda.felfel@nottingham.ac.uk; rmfelfel@mans.edu.eg

1 Division of Materials, Mechanics and Structures, Faculty of Engineering, University of Nottingham, Nottingham NG7 2RD, UK

2 Physics Department, Faculty of Science, Mansoura University, Mansoura 35516, Egypt

It is well known that the properties of polymers change significantly when they are above their glass transition temperature (T_g). Thus, accelerated degradation at a temperature range around the T_g (from below T_g to above T_g) may be required for an understanding of temperature-degradation dependence. There are not many studies where accelerated degradation was undertaken over such temperature ranges in order to explain the time–temperature equivalence of degradation [5].

Claes et al. [7] performed a comparison of the mechanical properties of PLA pins degraded in saline solution (NaCl) at 37 and 70 °C and compared them with the values of dry samples (non-degraded) obtained at 20 °C. The pins completely lost their flexural strength after 18 months at 37 °C, whereas strength was lost after only 96 h at 70 °C. They concluded that accelerated degradation tests can be afforded an expectation of degradation profiles in a short period of time (the results of the 70 °C test can be used to approximate the degradation behaviour at 37 °C). Poly (glycolide-co-L-lactide) (PGLA) multifilament braids were degraded in PBS media at five temperatures (from 27.5 to 47.5 °C with 5 °C increments) by Deng et al. [8]. The higher temperatures accelerated the degradation process significantly and caused a more rapid loss of tensile strength. The tensile strength of the braid was reported to decrease by 10 % after degradation in PBS media for 30 days at 37.5 °C. Similar percent of strength ($\sim$10 %) loss of the braid had also been reported after only 10 days degradation at 47.5 °C. The required time to reach a given breaking strength at different temperature was applied for Arrhenius equation and the activation energies were calculated (96.12–102.38 kJ mol^{-1}).

In this study, bioresorbable composites based on PLA and phosphate-based glass fibres (PGF) with different fibre orientation (random and unidirectional) within the composites were used. The degradation properties of the composites in PBS media were studied over six different temperatures (21, 37, 50, 65, 75 and 85 °C). The temperatures were selected to cover the range below and above the glass transition temperature (T_g) of dry PLA ($\sim$62 °C). The Arrhenius equation was applied and the activation energies for the degradation process were determined. Finally, predictive model for degradation at 37 °C was suggested based on the accelerated study.

Materials and methodology

Phosphate glass fibre (PGF) production

Continuous phosphate-based glass fibres were produced by melt spinning process using a dedicated in-house facility as reported previously by Felfel et al. [9, 10]. In brief, the glass was produced with the composition of 40P$_2$O$_5$–24MgO–16CaO–16Na$_2$O–4Fe$_2$O$_3$ (denoted as P40) in mol% using the sodium dihydrogen phosphate, calcium hydrogen phosphate, magnesium hydrogen phosphate trihydrate and iron phosphate dihydrate precursors (purchased from SigmaAldrich, UK). Specified amount of precursors were mixed and then preheated at 350 °C for 30 min before melting at 1100 °C for 90 min. The molten glass was poured directly onto a steel plate and allowed to cool to room temperature. The glass was kept in a desiccator until fibre production. Continuous fibres with around 15 µm diameter were produced by melting the glass at 1100 °C using a platinum crucible comprising a 0.2-mm hole at its base. The molten glass exited through the base of the crucible via the hole under the effect of gravity and was drawn downwards and collected on a drum using traverse mode and rotating at 1600 m min^{-1}. The fibres were annealed at 474 °C (which was 5 °C lower than the glass transition temperature of the glass) for 90 min prior to use to reduce the internal thermal stresses.

Preparation of non-woven random and continuous unidirectional fibre mats

Random non-woven mats (RM) were prepared using 10 mm chopped fibres. The fibres were separated into 3 g batches and dispersed in an aqueous solution of hydroxyethyl cellulose (0.003 % w/v) (Cellosize, HEC WP-52000HP, Dow Chemicals, Switzerland), which acted as a binder. Fibres were then stirred at 600 rpm for 10 min before extraction into randomly oriented fibre mats using a mesh strainer under vacuum. The RMs were then rinsed with deionised water to remove any residual binder before being dried at 50 °C for 30 min.

The unidirectional (UD) fibre mats were produced from 180-mm-long fibre bundles aligned together (manually) on a steel plate covered with Teflon sheet. Cellosize solution (0.003 % w/v) was added gently using a syringe in order to bind the fibres together. Two weights were used at the ends of fibres to keep the fibres straight. The UD mats were also rinsed with deionised water to remove any residual binder before being dried at 50 °C for 30 min.

Composites production

PLA films of approximately 0.2 mm thickness were produced via a compression moulding process. PLA beads (NatureWorks$^{®}$ 3251-D, average M_w $\sim$90,000–120,000, PDI = 1.636, melting temperature T_m = 170.9 °C, T_g = 62 °C) were melted at 210 °C for 10 min in between two metallic plates and then pressed at 3 bar for 30 s before being cooled down to room temperature (using a room temperature press) while retaining the same pressure.

Both the RM and UD composites were prepared via a film stacking process. The PLA films were stacked alternately with RMs in a 170 mm diameter, 2-mm-thick mould cavity between two metallic plates. Similar to PLA film production, the stack was heated in the press at 210 °C for 15 min and then pressed at 38 bar for 15 min followed by cooling down to room temperature at the same pressure. The same protocol was applied for the UD composite except that the mould cavity had dimensions of 160 mm × 160 mm × 2 mm. The fibre volume and mass fractions of the composites were obtained using the matrix burn-off method (see Table 1) according to the standard test method ASTM D2584-94 [11]. The target fibre volume fraction of the composites was between 18 and 20 %.

Differential scanning calorimetry (DSC)

DSC analysis was performed using a DSC Q10 (TA Instrument, USA) which was calibrated using indium. Samples ($\sim$6 mg) were placed into aluminium pans and heated over a temperature range from 30 to 190 °C at a rate of 10 °C min^{-1} under nitrogen gas flow (50 mL min^{-1}). Two heating cycles were used. After the first heating cycle, the sample was quenched at 20 °C min^{-1} to room temperature and the second scan performed immediately. The first run was applied to remove the thermal history of the samples [12]. All the samples were oven dried at 50 °C for 48 h prior to DSC analysis. The resulting thermograms were analysed using TA universal analysis 2000 software to determine the glass transition temperature (T_g), melting temperature (T_m) and the percentage of crystallinity ($X_c\%$). The second healing run was used to determine T_g and T_m values, whilst the crystallinity percentage was determined from the first run using the enthalpy of fusion for 100 % crystalline PLA (93.1 J g^{-1}) [13–15].

X-ray diffraction (XRD)

The X-ray diffraction (XRD) measurements were performed for PLA, RM and UD composites using a D500 diffractometer (SIEMENS). CuKa radiation ($\lambda = 0.154$ nm) was used at a voltage of 40 kV and current of 25 mA. The samples were scanned using a step-scanning method with a step-size of 0.05° and 2 s interval in the range from 10° to 35° of the diffraction angle (2θ).

Flexural test

Flexural strength and modulus values were determined at room temperature (20 °C) via three-point bending tests using a Hounsfield Series S testing machine. These measurements were performed according to the standards BS EN ISO 14125:1998 and BS 2782-10:1977 [16, 17]. Sample dimension of 40 mm × 15 mm × 2 mm, a crosshead speed of 1 mm min^{-1} and a 1 kN load cell were used. The measurements were conducted on wet samples after blot drying and in triplicate ($n = 3$).

Degradation study

The degradation study was performed according to the standard BS EN ISO 10993-13 [18]. Specimens of PLA, RM and UD composites were placed individually into 30 mL glass vials. The vials were filled with PBS media (pH 7.4 ± 0.2) and maintained at different degradation temperature (21, 37, 50, 65, 75 and 85 °C). At various time points (0, 1, 2, 3, 4, 6, 12, 15, 22, 29, 36, 43, 50 and 56 days) the specimens were extracted and blot dried before weighing. The samples were placed back into vials with fresh PBS solution at each time point. The average values were reported from at least three repeats. The percentage mass change and mass loss rate were determined using the following equations:

$$\text{Mass change} = \left(\frac{m - m_i}{m_i}\right) \times 100\,\% \tag{1}$$

$$\frac{\mathrm{d}}{\mathrm{d}t}(\text{Mass change}) = \frac{\left(\frac{m - m_i}{m_i}\right)}{t} \tag{2}$$

where m is the initial mass of the sample and m_i is the mass of degraded sample measured at time t.

Gel permeation chromatography (GPC)

The weight average molecular weight (M_w) of PLA in the specimens (PLA, RM and UD composites) was determined using gel permeation chromatography (GPC), which was performed using a refractive index (RI) detector and with HPLC grade chloroform (Fisher Scientific, UK) as a solvent. Analysis was performed at 40 °C with a flow rate of 1 mL min^{-1} through two PLgel Mixed-C columns with a calibration range of 5000–300,000 Da calibrated with

Table 1 Fibre volume fractions, mass fractions and sample codes for the composites

Composite code	Specimen	Fibre volume fraction (%)	Fibre mass fraction (%)
PLA	PLA alone	N/A	N/A
P40 RM	PLA–PBG random mat composite	18 ± 3	34 ± 4
P40 UD	PLA–PBG random mat composite	14 ± 2	26 ± 3

polystyrene narrow standards. All GPC equipments and standards were supplied by Polymer Laboratories (Varian Inc). GPC data was analysed using the Cirrus GPC Offline software package version 3.0.

Arrhenius equation

The Arrhenius equation represents the effect of temperature on a reaction rate [19, 20].

$$k = Ae^{-E_a/RT} \tag{3}$$

where k is reaction rate, A is constant, E_a is the activation energy (cal), R is universal gas constant (J K^{-1} mol^{-1}) and T is the temperature in Kelvin. If the Arrhenius equation is applicable for the degradation results, a linear relation should exist between ln K and 1/T.

$$\ln K = -\left(\frac{E_a}{R}\right)\left(\frac{1}{T}\right) + \ln A \tag{4}$$

Scanning electron microscopy (SEM)

Specimens were prepared by freeze fracture using liquid nitrogen. They were sputter-coated with carbon and examined using a JEOL 6400 SEM with an accelerating voltage of 10 kV in secondary electron mode (SE).

Results and discussion

The complete degradation of bioresorbable polymeric devices takes a considerable length of time at physiological temperature (37 °C). Therefore, accelerated degradation would enable savings of time as well as research funds. The results obtained from accelerated degradation could be extrapolated to predict the behaviour of the device at body temperature. The degradation process could be accelerated using monolayer of the specimen [21, 22], pH and/or temperature of the degradation medium [23]. This study focuses on the use of a temperature accelerated degradation

system. Weir et al. [24] reported that the results acquired from degradation above the T_g for semi-crystalline polymers were still valid for prediction of properties below the T_g and therefore, a continuous relationship has been assumed over the temperature ranges from 21 to 85 °C.

Thermal and crystalline properties

The thermal properties for PLA before and after degradation in PBS media at different temperatures are presented in Table 2. As overall trend, glass transition (T_g) and melting temperatures (T_m) of the PLA were seen to decrease and consequently the crystallinity were found to increase when degraded in PBS media with the increasing conditioned temperature. Before the degradation, the initial T_g and T_m were observed to be around 61.3 and 167.4 °C, respectively. There was no significant change in their T_g and T_m values ($P > 0.05$) after degradation in PBS at 21 or 37 °C. However, a significant decrease in T_g and T_m by approximately 9 and 14 °C ($P < 0.05$), respectively, were observed after degradation in PBS at higher temperatures (50, 65, 75 and 85 °C). This was suggested to be due to a reduction in the molecular weight and partial degradation of crystalline phase after the amorphous regions were exhausted [25–27]. The percentage crystallinity of PLA increased with increasing degradation at temperatures (see Table 2). This increase was attributed to a combination of the plasticisation and a more rapid degradation of the amorphous regions of the polymer, in comparison to the crystalline regions [9, 12, 28]. During the degradation of PLA, water diffuses into the amorphous regions initially, which are less packed and allow water penetration more easily than the crystalline regions. After the degradation of most or all the amorphous regions, the water slowly penetrates into the crystalline regions. Therefore, the crystallinity could be decreased as the crystalline parts were also affected by diffusion of water molecules [29].

The crystallinity of the PLA were further characterised via XRD analysis, where Fig. 1 reveals the XRD patterns of PLA specimens before and after degradation in PBS

Table 2 Thermal properties of PLA after degradation in PBS at different temperatures

Temperature (°C)	Degradation period (days)	Glass transition temperature T_g (°C)	Melting temperature T_m (°C)	Crystallinity (%)
Before degradation	0	61.3 ± 0.2	167.4 ± 1.2	9.2 ± 0.4
21	56	61.7 ± 0.4	169.9 ± 0.8	13.4 ± 0.7
37	56	60.9 ± 0.3	167.8 ± 0.5	11.8 ± 1.9
50	56	52.2 ± 0.7	154.2 ± 0.6	41.8 ± 1.3
65	12	52.2 ± 0.5	154.4 ± 0.7	61.2 ± 0.9
75	6	52.4 ± 0.7	155.0 ± 1.1	58.8 ± 2.3
85	3	52.7 ± 0.2	151.6 ± 0.8	58.3 ± 0.9

Fig. 1 XRD pattern for PLA before and after degradation in PBS for varying time points (0, 3, 6, 12 and 56 days) obtained at different temperatures (21, 37, 50, 65, 75 and 85 °C)
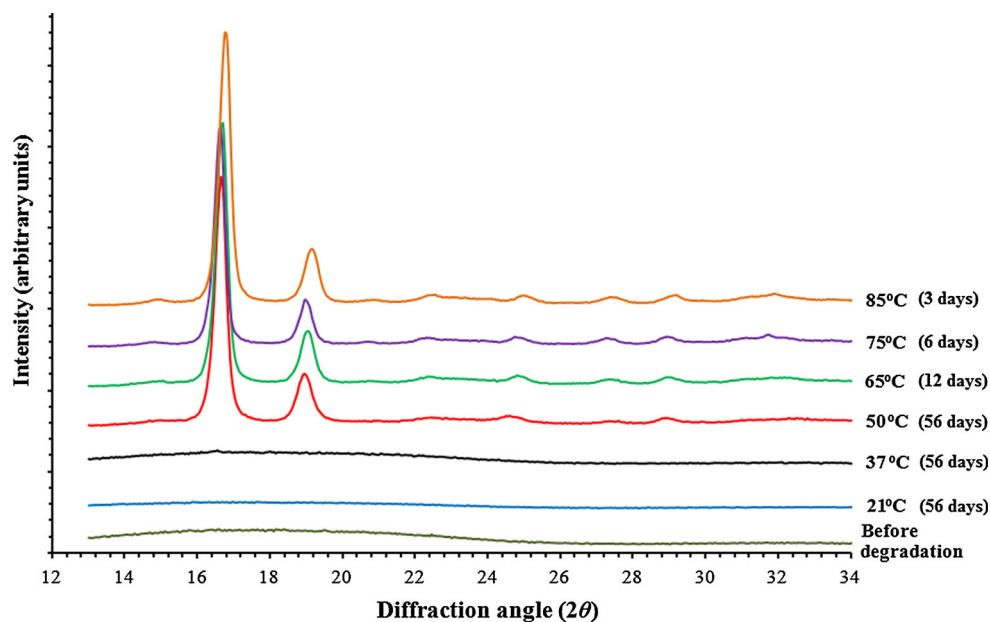
media at different temperatures (0, 3, 6, 12 and 56 days). No sharp diffraction peaks are detected before and after degradation in PBS at 21 and 37 °C. However, after degradation at the higher temperatures (50, 65, 75 and 85 °C), two sharp peaks were detected at $2\theta = 16.5°$ and 19°, which correlates well with the crystallinity data obtained via DSC scans. This was again suggested to be due to the increasing portion of crystalline phases within the

polymer chain after degradation of most of the amorphous phases [26, 27, 30].

SEM analysis

Figures 2 and 3 show the fracture surfaces for P40 RM and P40 UD composite specimens before and after degradation at different temperatures (21, 37 and 65 °C). SEM
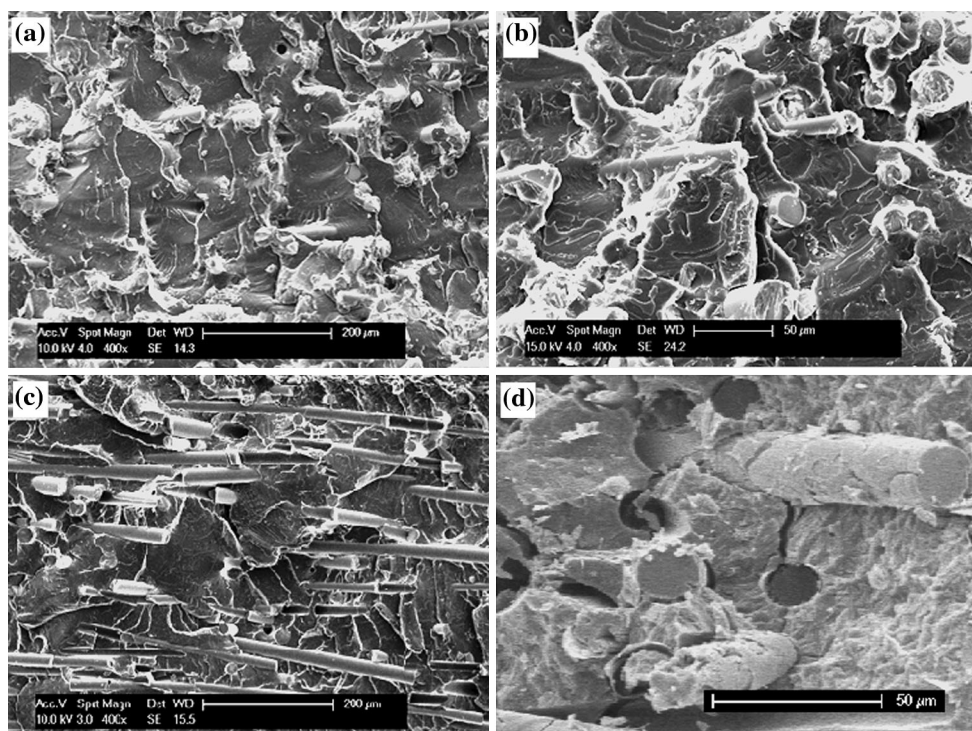

Fig. 2 SEM micrographs of a freeze-fractured surface for P40 RM composites **a** before degradation, **b** after 56 days of degradation at 21 °C, **c** after 56 days of degradation at 37 °C and **d** after 12 days of degradation at 65 °C
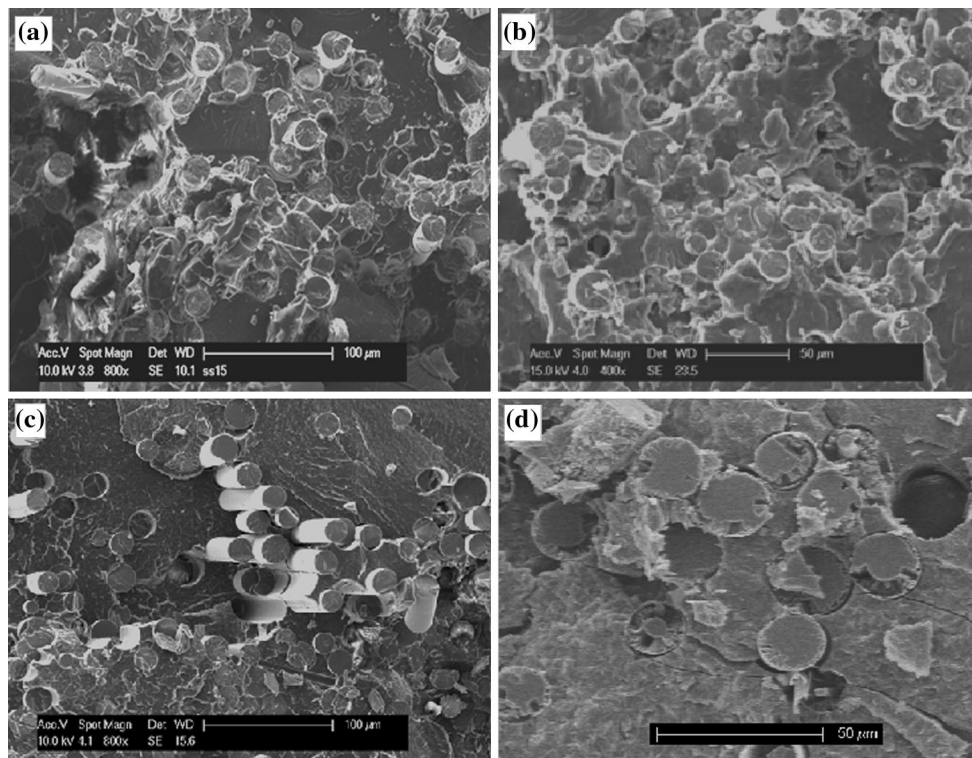
Fig. 3 SEM micrographs of a freeze-fractured surface for P40 UD composites **a** before degradation, **b** after 56 days of degradation at 21 °C, **c** after 56 days of degradation at 37 °C and **d** after 12 days of degradation at 65 °C

micrographs for degraded composites at elevated temperatures (50, 65, 75 and 85 °C) were similar (data not shown here). Therefore, specimens after degradation at 65 °C were selected as an example. Degradation effects can be seen on the fibre surfaces (see Figs. 2, 3) as pitting and cracks which were suggested to be due to accelerated degradation at elevated temperature (65 °C). The cracks could also be attributed to the ion exchange with the degradation medium [31].

Flexural properties

The flexural properties for PLA alone, P40 RM and P40 UD composites before and after degradation in PBS at different temperatures are shown in Fig. 4. No significant changes ($P > 0.05$) in flexural strength and modulus were observed between initial properties and those after degradation in PBS media at 21 °C for 56 days, although a slight increase in the modulus for PLA was apparent. This could be due to the persistence of the fibre-matrix interface as seen from the SEM micrographs (see Figs. 2b, 3b).

After 56 days of degradation in PBS at 37 °C, the flexural strength decreased by approximately 20 % for PLA and around 50 % for the both type of composites (UD and RM). However, a little change was seen for the flexural modulus values except for the RM composites, which fell

by ~45 %. After degradation at 37 °C short fibre pull-out and clean fibre surfaces were observed, which are indicative of degradation of the fibre-matrix interface (see Figs. 2c, 3c). The flexural strength and modulus values for all the samples decreased dramatically after 56 days of degradation in PBS at 50 °C. Samples degraded in media at temperatures higher than 50 °C were so fragile that they broke before flexural testing could be performed. Inequality in flexural strength and modulus for PLA, P40 RM and P40 UD composites after degradation at up to 50 °C in PBS was suggested to be due to a number of factors; (i) ability of water to penetrate the network at higher temperature due to higher chain mobility, (ii) an increase in the degradation rate of the matrix as well as the fibre-matrix interface as the degradation temperature increased, (iii) as the temperature became close to the glass transition temperature of the matrix, the fibre-matrix interfacial shear strength decreased [32] and (iv) degradation of the fibres at elevated temperatures [31]. Chin et al. [33] studied the effect of ageing in deionised water at different temperatures (room temperature, 40, 60 and 80 °C) on the interlaminar shear strength of glass fibre reinforced vinyl ester and isophthalic polyester composites. They found that the interlaminar shear strength for vinyl ester composites ($T_g = 78$ °C) was less susceptible to degradation in water at different temperatures than that for isophthalic polyester

Fig. 4 Flexural properties for PLA, P40 RM and P40 UD composites before and after degradation in PBS at different temperatures; **a** flexural strength and **b** flexural modulus. *One sample was tested because the other two replicates were broken before the flexural test
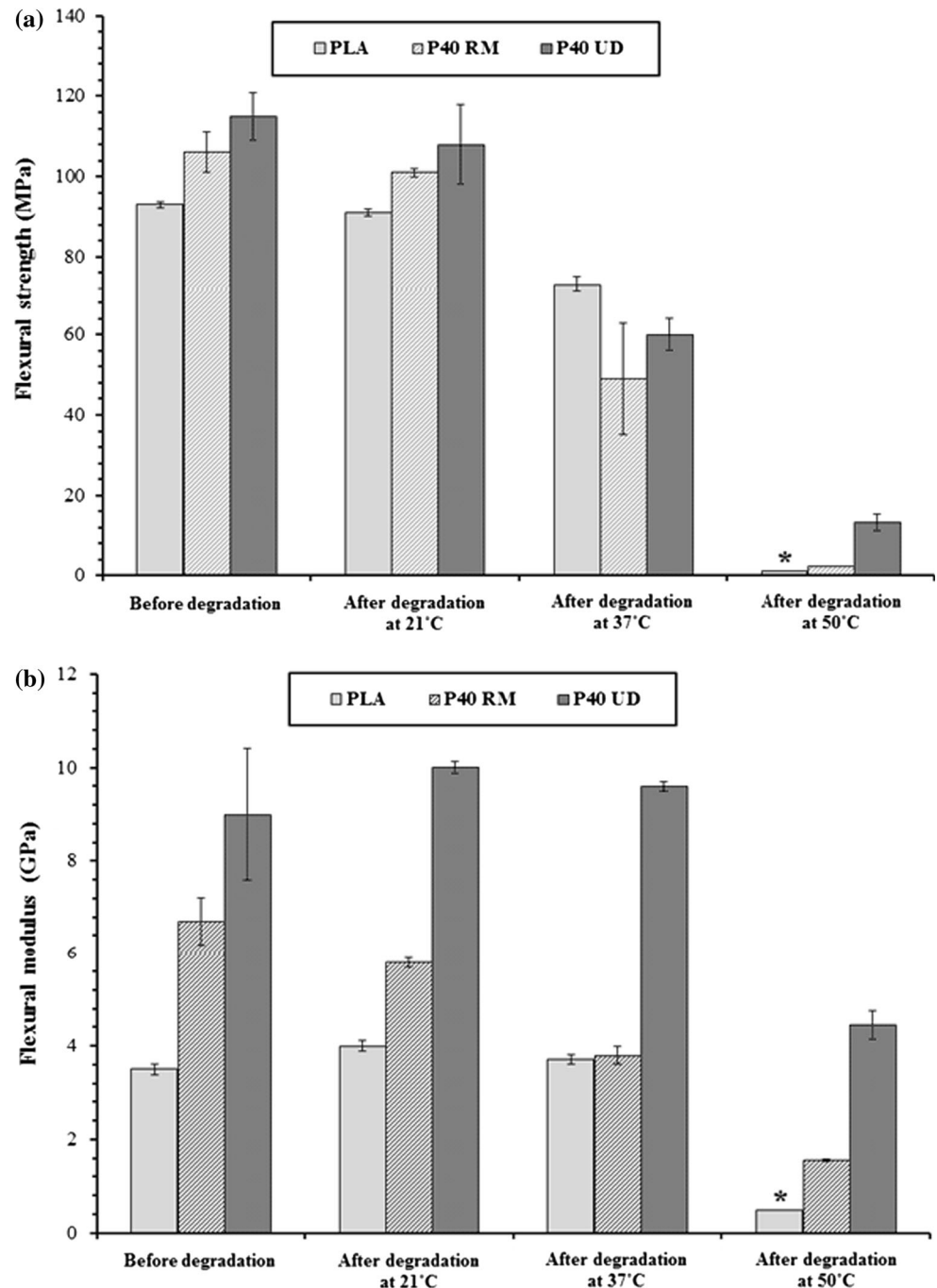
composites ($T_g = 132$ °C). This could be due to their differences in T_g values; as they suggested that the degradation rate was higher when the conditioned temperature approached to their T_g values.

During the degradation of the composites in PBS at elevated temperatures (above 50 °C), a drastic reduction in their flexural properties was observed. This was attributed to be due to the partial degradation of the matrix and fibres and a complete degradation of the fibre-matrix interfaces,

which can also be seen in the SEM images (see Figs. 2d, 3d).

Degradation study

Figure 5a–c show percentage change in mass (wet basis) against time at different temperatures for PLA alone, P40 RM and P40 UD composites. The wet mass change profile can be divided into three regions; an initial increase as a
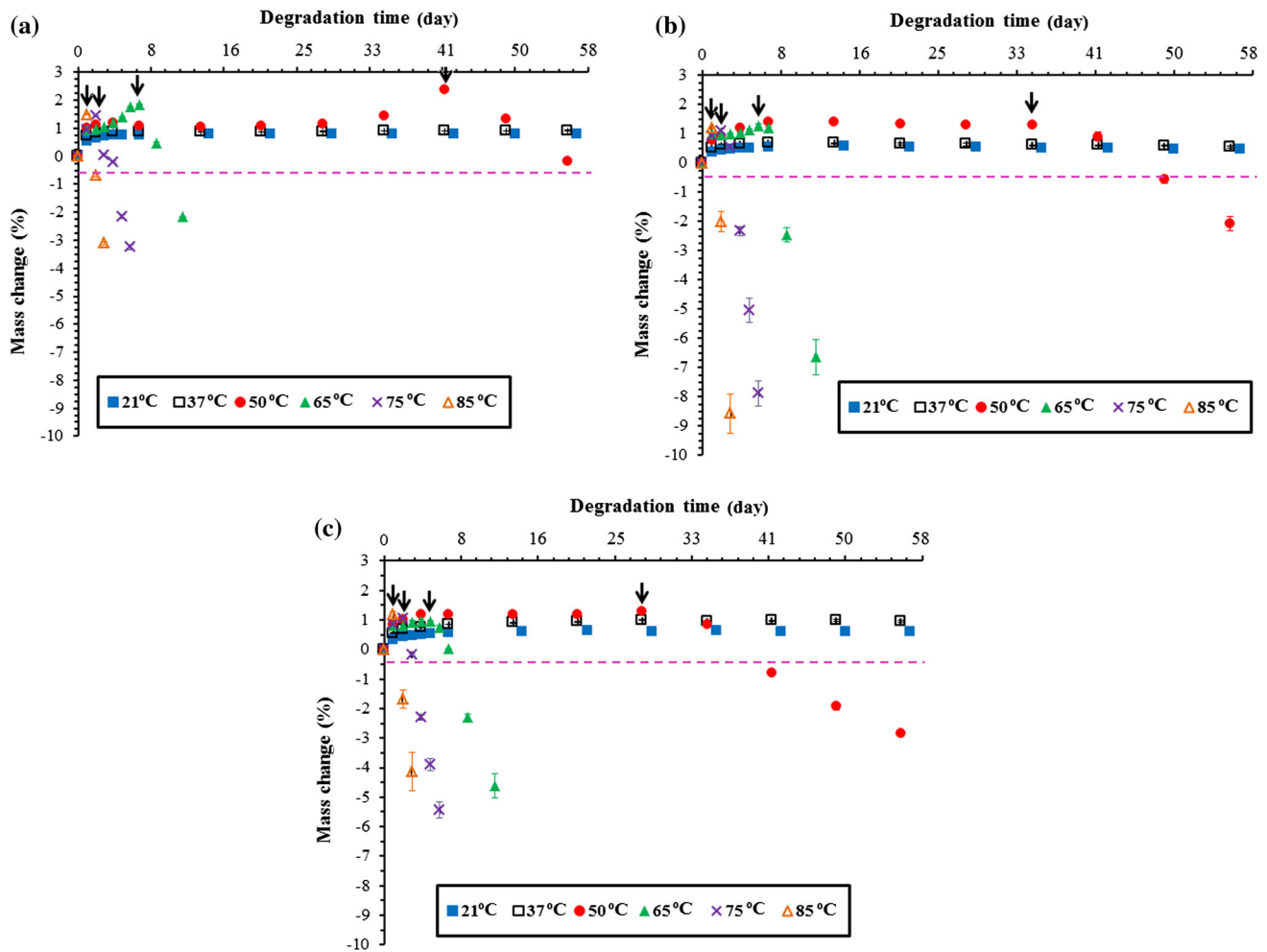
Fig. 5 Percentage of mass change against time during degradation in PBS at different temperatures (21, 37, 50, 65, 75 and 85 °C) for **a** PLA alone, **b** P40 RM and **c** P40 UD composites. *Arrows* in the figures refers to the tipping time for each specimen at different temperatures

result of water uptake, a plateau after saturation and then a final decrease due to mass loss. The three regions are clear for degradation at 50 °C. The saturation region size decreased with increasing degradation temperature, completely disappearing by 75 °C. In addition, the size of plateau increased with decreasing temperature at 21 and 37 °C where no measurable mass loss was observed till the end of study. Further degradation at 21 and 37 °C (more than 1 year) was required to detect drop in the wet mass. During degradation at 21 and 37 °C, the mass increased initially to ~0.5 and ~0.7 % for PLA, P40 RM and P40 UD composites at 21 and 37 °C, respectively, and then levelled off till the end of degradation period. At 50 °C, PLA, P40 RM and P40 UD composites saturated at ~1 % for ~900, 800 and 700 h, respectively. The masses decreased to ~−0.2 % for PLA alone and ~−2.8 % for the composites by the end of degradation period at 50 °C. Similar degradation profiles were seen during degradation

in PBS media at temperatures above the T_g of PLA ($T_g = 62$ °C) with shorter saturation periods.

Change in mass of specimens was influenced by water uptake and mass loss. During the initial period, wet mass of the samples increased gradually until saturation as a result of predominant of water uptake over mass loss. Balance between mass loss and water uptake was the main reason for saturation. After the tipping point, mass loss became superior over water uptake resulting in drop in wet mass change. The significant decrease in wet mass was observed at specific times (tipping time point, see Fig. 5) during degradation in PBS at 50 °C and above. Tipping point was not noticeable for degradation at 21 and 37 °C as the degradation period was insufficiently long. The decrease in mass at this time (tipping point time) was attributed to the polymer achieving a critical molecular weight, sufficiently small to allow diffusion out of the bulk of the matrix. The tipping time became shorter as the degradation temperature
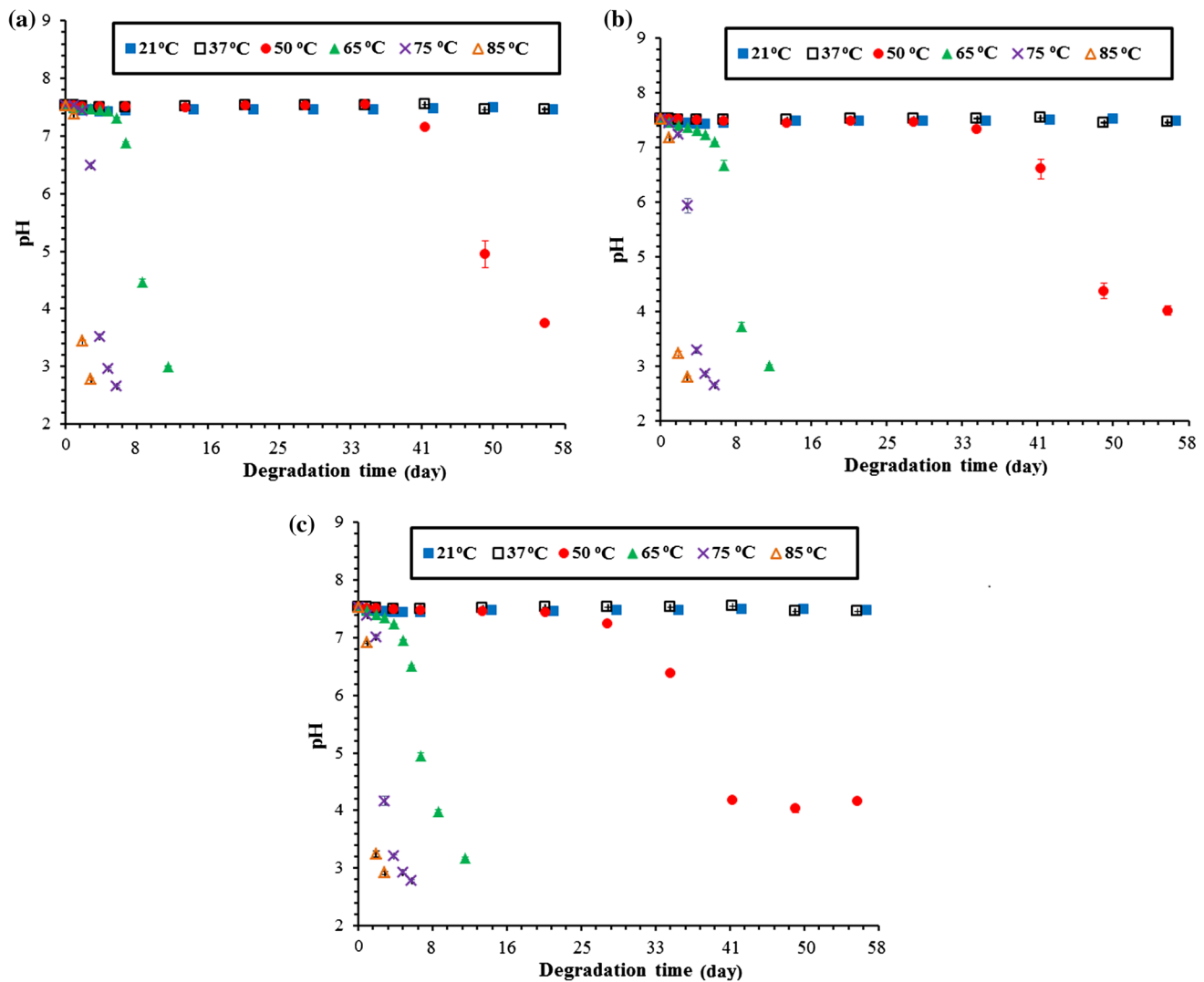
Fig. 6 pH change for PBS during immersion in PBS at different temperatures (21, 37, 50, 65, 75 and 85 °C) for **a** PLA alone, **b** P40 RM and **c** P40 UD composites

increased due to the fact that the hydrolysis process was accelerated by increasing the temperature [5].

Figure 6a–c provides the changes in pH of degradation medium against time. There was a good correlation between wet mass change and pH change against time (as expected since the degradation products of PLA and phosphate glass are acidic) [6]. Values of pH remained neutral (~7.4) for all specimens degraded at 21 and 37 °C. During degradation at higher temperatures, the pH of PBS remained constant for certain periods before decreasing and the length of the pH compensation periods decreased as the incubation temperature increased. There was no significant difference in the pH profiles for PLA, P40 RM composites. Whilst for P40 UD composites, the pH change was slightly faster than that for PLA and P40 RM composites (see Fig. 6c). Lyu et al. [5, 19] suggested the

mechanism of degradation process for PLA; (i) firstly, water diffusion into the polymer until saturation (within 2–3 days), (ii) then degradation with constant rate which depends on the water uptake, (iii) accelerated hydrolysis as a result of production of chain ends in the degradation medium, and lastly (iv) significant increase in water uptake and mass loss due to dissolution of the degraded chains in the water.

Molecular weight distribution

Figure 7 shows GPC curves representing the molecular weight distribution of PLA before and after degradation in PBS at different temperatures. The molecular weights of PLA composites decreased after degradation at different

Fig. 7 Molecular weight distribution for PLA before and after degradation in PBS for varying time points (0, 3, 6, 12 and 56 days) obtained at different temperatures
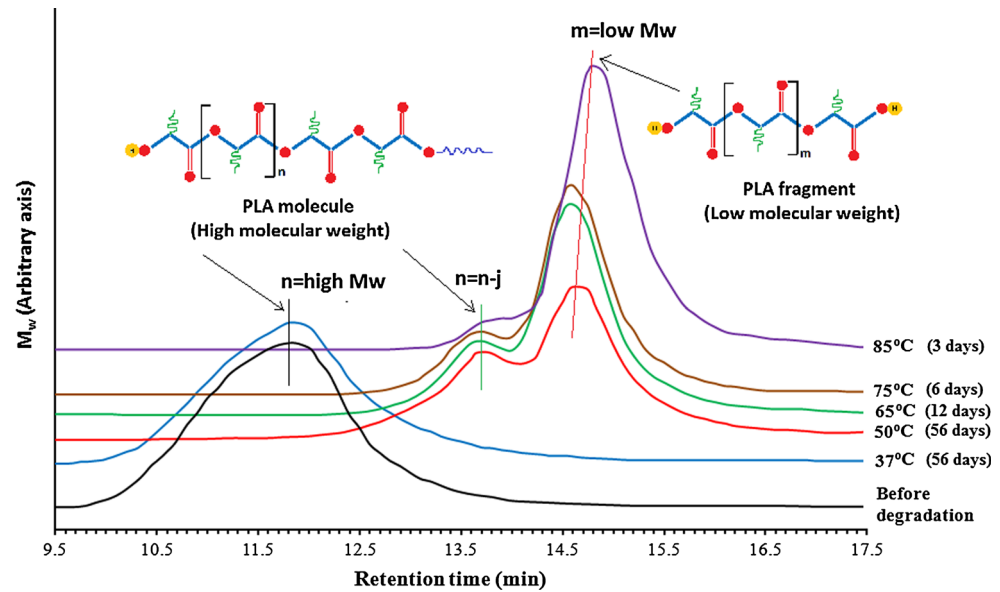
temperatures. As expected, the reduction in molecular weight became more pronounced as the degradation temperature increased. During the degradation process, molecular weight decreased due to chain scission via autocatalytic hydrolysis [9, 10, 34]. The molecular weight distribution of PLA after degradation in PBS at 21 and 37 °C was seen to be monomodal and located at the left of GPC curves (see Fig. 7), which was suggested to be due to the domination of high molecular weight chains of PLA. However, at higher temperature (above 37 °C) the GPC curves became bimodal and also shifted to the right. This indicated the presence of both low and high molecular weight degraded PLA fragments [35]. The sharp peaks in the bimodal GPC curves located to the right suggested the presence of comparatively higher amount of low molecular weight chains. On the other hand, the small peaks observed on the left of the sharp peaks in the bimodal curves were attributed to the existence of fewer high molecular weight fragments. However, the molecular weight of the chains obtained from the bimodal GPC curves (for the degraded PLA conditioned at higher temperature) was believed to be much lower than that of obtained from the monomodal GPC curves. Bimodal distributions were attributed to the variation in degradation rate between amorphous and crystalline phases within semi-crystalline polymers, faster internal degradation at elevated degradation temperatures and crystallisation of degradation products retarding further degradation [3, 25, 30].

Figure 8a illustrates molecular weight distribution for the PLA, P40 RM and P40 UD composites after degradation at 50 °C for 8 weeks. All specimens showed bimodal pattern and peaks shifted towards lower molecular weight for P40 UD composites. Schematic diagrams for degradation process of P40 UD and P40 RM composites are shown

in Fig. 8b, c. It can be illustrated that degradation rate for P40 UD composites was faster than that for P40 RM. This is suggested to be due to that the speed of water wicking at unidirectional fibre/matrix interfaces is faster than the random fibre mats. Discontinuous nature of the fibres within P40 RM composites makes them less prone to water wicking [36]. The influence of fibre orientation on diffusion of water was also presented by Arnold et al. [37]. They concluded that water diffused along the fibres faster than in other directions [38].

Calculation of activation energy

Applying the Arrhenius equation (Eq. 3) to the rate of change in molecular weight of the polymer and composite samples yielded linear relationships in each case (Fig. 9a–c). The degradation activation energies were calculated from the gradient of the linear relations. The degradation activation energies were calculated to be 85.4, 78.7 and 74.1 kJ mol^{-1} for PLA within PLA alone, P40 RM and P40 UD composites, respectively. Weir et al. [24] and Agrawal et al. [6] studied the change in molecular weight against degradation temperature over a range of temperatures (below to above T_g). They found that activation energies for 50 %PLA–50 %PGA copolymer and PLLA were 113.9 and 100.5 kJ mol^{-1}, respectively. Pietrzak et al. [2] applied the Arrhenius equation to determine the degradation activation enthalpy using a change in inherent viscosity for a 52 %PLLA–18 %PGA copolymer ($T_g = 55$ °C). They conducted the investigation over a temperature range from 4 to 49.3 °C and the activation energy was found to be 100.1 kJ mol^{-1}. Degradation activation energy for 10 %PLLA–90 %PGA was determined by the change in tensile breaking strength retention vs degradation time in
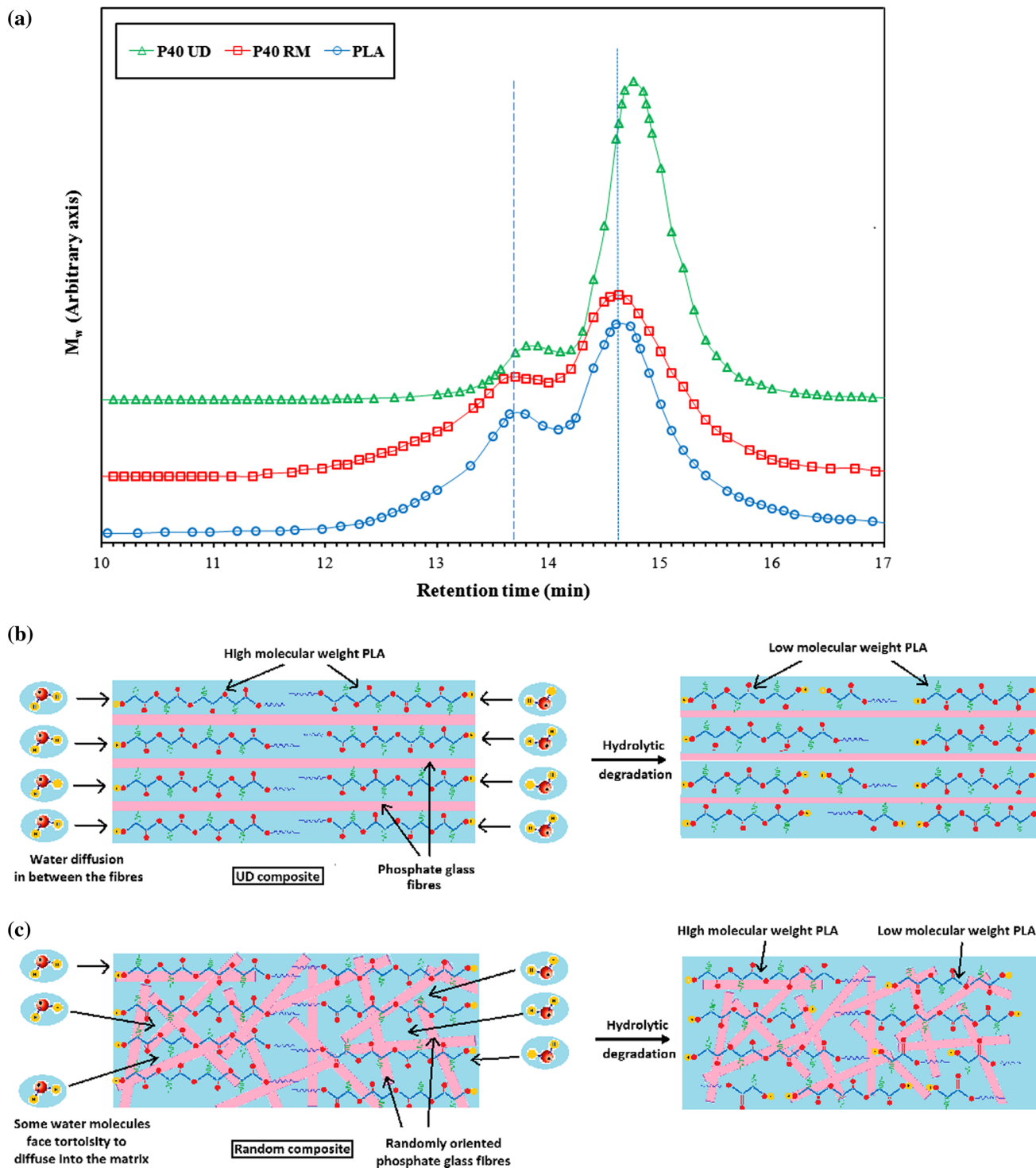
(a)

(b)

(c)

Fig. 8 **a** Molecular weight distribution for PLA, P40 RM and P40 UD composites after degradation at 50 °C for 56 days. Scheme of degradation mechanism for **b** P40 UD composites, and **c** P40 RM composites

PBS at different temperatures (27.5, 32.5, 37.5, 42.5, 47.5 °C) [8]. The activation energy that was obtained ranged between 95.9 and 102.6 kJ mol^{-1}. In this study, degradation activation energy was determined by the change of molecular weight against temperature and the values were obtained in between 74.1 and 85.4 kJ mol^{-1}. The activation energy for PLA was slightly lower than the published values [24] as the initial molecular weight and crystallinity were 4–5 times higher than that of the PLA used in the current study.
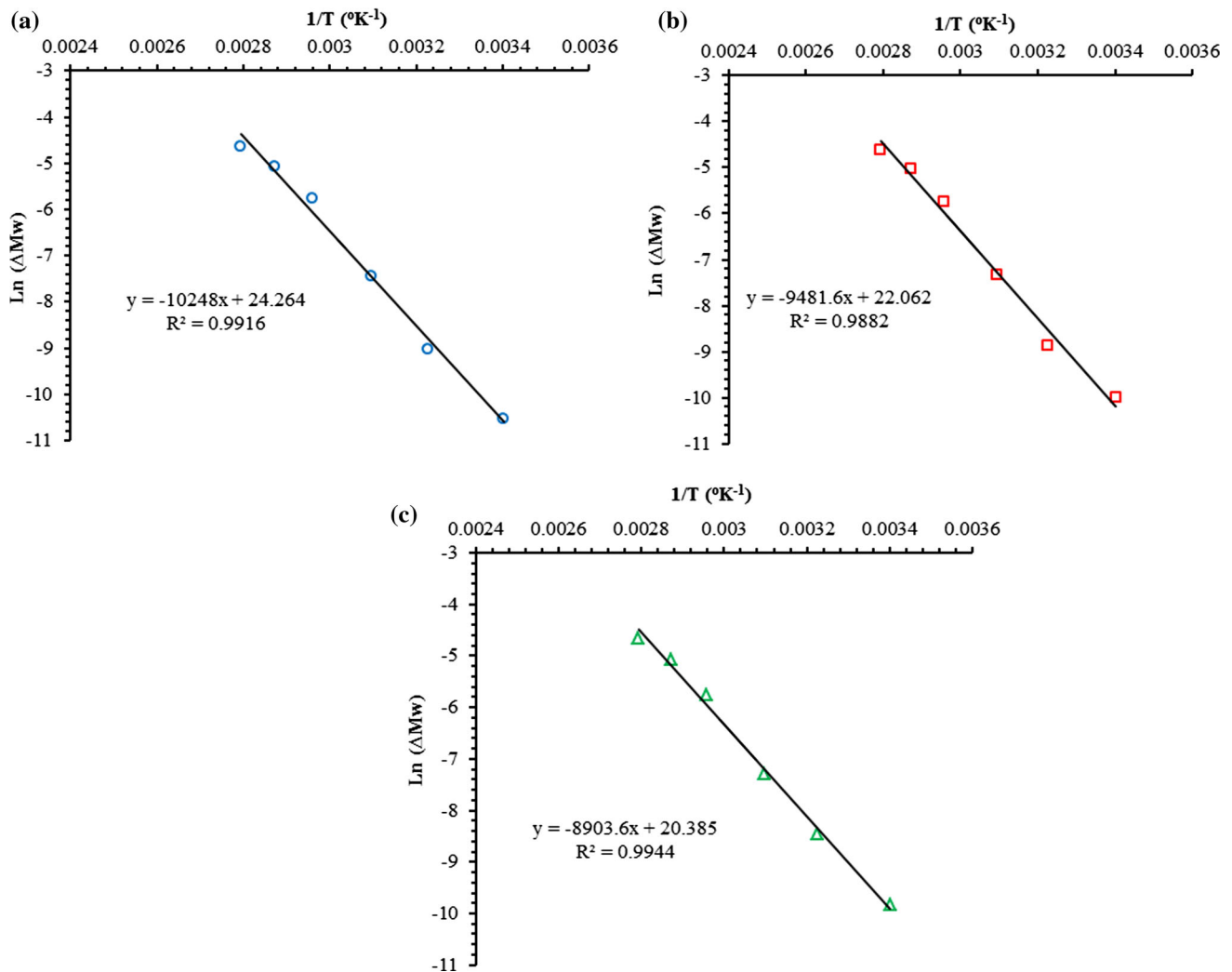
Fig. 9 Arrhenius relation for rate of molecular weight loss against temperature during degradation in PBS at different temperatures for **a** pure PLA, **b** P40 RM composites and **c** P40 UD composites

Prediction of long-term effects

Time prediction was applied to correlate short-term degradation (at elevated temperatures) to the long-term effects (at 37 °C). Power equations were obtained by fitting plots relating degradation temperature to the tipping time point (the time at which the mass of specimens began to decrease, see Fig. 5). Figure 10 shows a linear relation between tipping time and degradation temperature for pure PLA, P40 RM and P40 UD composites, respectively.

Figure 11 shows the half-life of molecular weight (M_w $t_{1/2}$) (i.e. required time for molecular weight to fall to half its value) against temperature for pure PLA, P40 RM and P40 UD composites during degradation in PBS at different temperatures. Fitting M_w $t_{1/2}$ vs degradation temperature (T) shows a linear relationship. The procedure reported by Litherland et al. [39] was applied. Molecular weight change against degradation time was used in this study because

molecular weight decreases linearly with the time [9, 10, 14, 40]. The two predictive methods (see Figs. 10, 11) provided very similar results. Potentially, both of them are applicable for time correlation and prediction, though the method in Fig. 11 is arguably a simpler method to use experimentally.

Conclusion

Degradation properties for PLA, P40 RM and P40 UD solid composites such as change in mass, pH and molecular weight with time can be accelerated by increasing the degradation temperature as expected. No statistically significant change in their T_g and T_m values after degradation in PBS at 21 or 37 °C were observed. A significant decrease in T_g and T_m by approximately 9 and 14 °C, respectively, and consequently a significant increase in their crystallinity were observed after degradation in PBS at higher temperatures (50, 65, 75 and

Fig. 10 Relation between degradation temperature and tipping time point (at which the mass of specimen began decrease) for PLA alone, P40 RM and P40 UD composites during the degradation in PBS
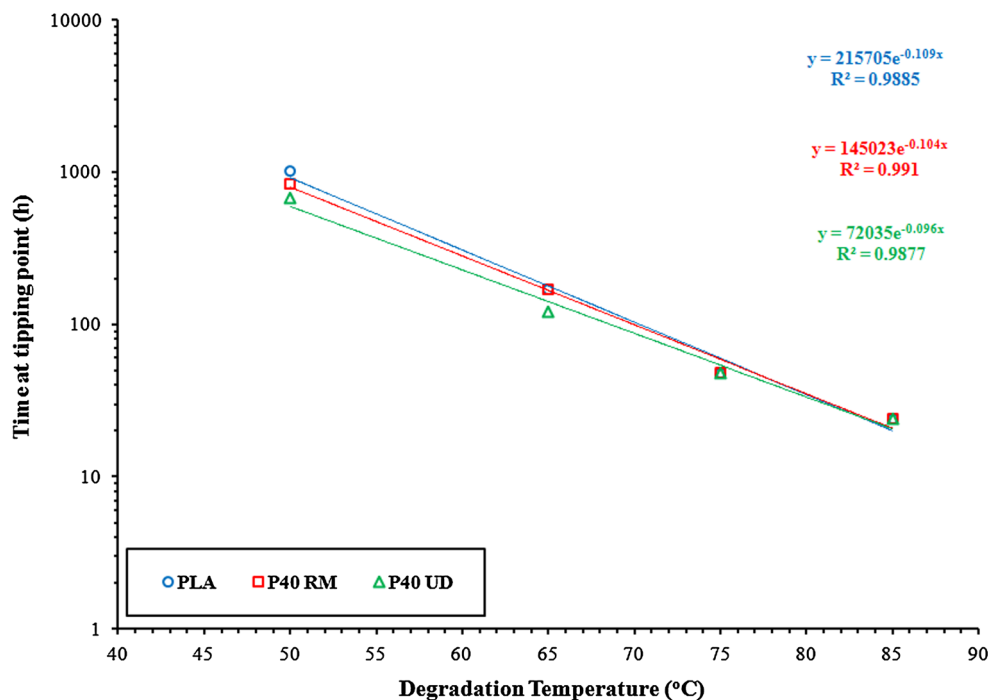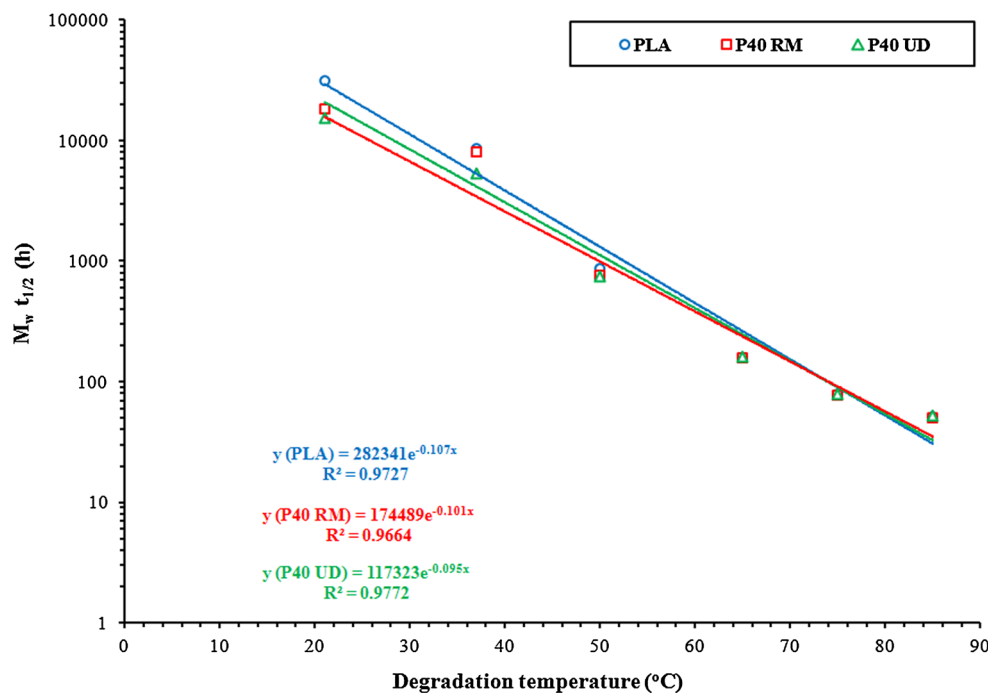

$$y = 215705e^{-0.109x}$$
$$R^2 = 0.9885$$

$$y = 145023e^{-0.104x}$$
$$R^2 = 0.991$$

$$y = 72035e^{-0.096x}$$
$$R^2 = 0.9877$$

Fig. 11 Molecular weight half-life vs degradation temperature for pure PLA, P40 RM and P40 UD composites during degradation in PBS at different temperatures

$$y\,(\text{PLA}) = 282341e^{-0.107x}$$
$$R^2 = 0.9727$$

$$y\,(\text{P40 RM}) = 174489e^{-0.101x}$$
$$R^2 = 0.9664$$

$$y\,(\text{P40 UD}) = 117323e^{-0.095x}$$
$$R^2 = 0.9772$$

85 °C) due to a reduction in the molecular weight and degradation of the amorphous regions of polymer chain. In addition, significant decreases in flexural properties of the UD and RM composites were observed to be much higher compared to the control PLA, which demonstrated the faster degradation of the fibre/matrix interfaces. Furthermore, the change of the molecular weight distribution with temperature within the degraded composites obeyed the Arrhenius equation and the degradation activation energies were obtained in the range of 74.1–85.4 kJ mol^{-1}. Linear relationship between the tipping time of the mass change and half-life of the molecular weight change vs incubation temperature were also justified, which could potentially be used to extrapolate short-term accelerated degradation effects to predict the long-term

degradation properties of solid composites at physiological temperature. Further work needs to be investigated to validate for porous materials.

References

1. Athanasiou KA et al (1998) Orthopaedic applications for PLA-PGA biodegradable polymers. Arthroscopy 14(7):726–737
2. Pietrzak WS, Kumar M, Eppley BL (2003) The influence of temperature on the degradation rate of LactoSorb copolymer. J Craniofac Surg 14(2):176–183
3. Li S (1999) Hydrolytic degradation characteristics of aliphatic polyesters derived from lactic and glycolic acids. J Biomed Mater Res 48(3):342–353
4. Ashammakhi N, Rokkanen P (1997) Absorbable polyglycolide devices in trauma and bone surgery. Biomaterials 18(1):3–9
5. Lyu SP et al (2007) Kinetics and time–temperature equivalence of polymer degradation. Biomacromolecules 8(7):2301–2310
6. Agrawal CM et al (1997) Elevated temperature degradation of a 50:50 copolymer of PLA-PGA. Tissue Eng 3(4):345–352
7. Claes LE et al (1996) New bioresorbable pin for the reduction of small bony fragments: design, mechanical properties and in vitro degradation. Biomaterials 17(16):1621–1626
8. Deng M et al (2005) Effect of load and temperature on in vitro degradation of poly(glycolide-co-L-lactide) multifilament braids. Biomaterials 26(20):4327–4336
9. Felfel RM et al (2012) Investigation of crystallinity, molecular weight change, and mechanical properties of PLA/PBG bioresorbable composites as bone fracture fixation plates. J Biomater Appl 26(7):765–789
10. Felfel RM et al (2011) In vitro degradation, flexural, compressive and shear properties of fully bioresorbable composite rods. J Mech Behav Biomed Mater 4:1462–1472
11. ASTM Standard D2584-94 (1994) Standard test method for ignition loss of cured reinforced resins
12. Buchanan FJ (ed) (2008) Degradation rate of bioresorbable materials prediction and evaluation. Woodhead Publishing Ltd, Cambridge, p 320
13. Navarro M et al (2005) In vitro degradation behavior of a novel bioresorbable composite material based on PLA and a soluble CaP glass. Acta Biomater 1(4):411–419
14. Tsuji H, Ikarashi K (2004) In vitro hydrolysis of poly(l-lactide) crystalline residues as extended-chain crystallites: II. Effects of hydrolysis temperature. Biomacromolecules 5(3):1021–1028
15. Lee TH, Boey FYC, Khor KA (1995) On the determination of polymer crystallinity for a thermoplastic PPS composite by thermal analysis. Compos Sci Technol 53(3):259–274
16. BS EN ISO 14125 (1998) Fiber reinforced plastic composites—Determination of flexural properties. Geneva, Switzerland
17. BS EN ISO 1008B (1996) Methods of testing plastics. Part 10: glass reinforced plastics method 1008B: determination of flexural strength on rods made of roving-reinforced resin
18. BS EN ISO 10993-13 (2010). Biological evaluation of medical devices. Identification and quantification of degradation products from polymeric medical devices
19. Lyu S, Untereker D (2009) Degradability of polymers for implantable biomedical devices. Int J Mol Sci 10(9):4033–4065
20. Han X et al (2010) Analysis of degradation data of poly(l-lactide-co-l, d-lactide) and poly(l-lactide) obtained at elevated and physiological temperatures using mathematical models. Acta Biomater 6(10):3882–3889
21. Tsuji H, Tsuruno T (2010) Accelerated hydrolytic degradation of poly(l-lactide)/poly(d-lactide) stereocomplex up to late stage. Polym Degrad Stab 95(4):477–484
22. Lee W-K, Iwata T, Gardella JA (2005) Hydrolytic behavior of enantiomeric poly(lactide) mixed monolayer films at the air/water interface: stereocomplexation effects. Langmuir 21(24):11180–11184
23. Xu L, Crawford K, Gorman CB (2011) Effects of temperature and pH on the degradation of poly(lactic acid) brushes. Macromolecules 44(12):4777–4782
24. Weir N et al (2004) Degradation of poly-L-lactide. Part 2: increased temperature accelerated degradation. Proc Inst Mech Eng [H] 218(5):321–330
25. Weir N et al (2004) Degradation of poly-L-lactide. Part 1: in vitro and in vivo physiological temperature degradation. Proc Inst Mech Eng [H] 218(5):307–319
26. Yuan X, Mak AFT, Yao K (2002) Comparative observation of accelerated degradation of poly(l-lactic acid) fibres in phosphate buffered saline and a dilute alkaline solution. Polym Degrad Stab 75(1):45–53
27. Li S, Garreau H, Vert M (1990) Structure–property relationships in the case of the degradation of massive poly(α-hydroxy acids) in aqueous media. J Mater Sci Mater Med 1(4):198–206. doi:10.1007/BF00701077
28. Li SM, Garreau H, Vert M (1990) Structure–property relationships in the case of the degradation of massive aliphatic poly-(α-hydroxy acids) in aqueous media. J Mater Sci Mater Med 1(3):123–130
29. Hakkarainen M, Albertsson A-C, Karlsson S (1996) Weight losses and molecular weight changes correlated with the evolution of hydroxyacids in simulated in vivo degradation of homo- and copolymers of PLA and PGA. Polym Degrad Stab 52(3):283–291
30. Li S, McCarthy S (1999) Further investigations on the hydrolytic degradation of poly (DL-lactide). Biomaterials 20(1):35–44
31. Karbhari VM (2004) E-glass/vinylester composites in aqueous environments: effects on short-beam shear strength. J Compos Constr 8(2):148–156
32. Straub A, Slivka M, Schwartz P (1997) A study of the effects of time and temperature on the fiber/matrix interface strength using the microbond test. Compos Sci Technol 57(8):991–994
33. Chin JW, Hughes WL, Signor A (2001) Elevated temperature aging of glass fiber reinforced vinyl ester and isophthalic polyester composites in water, salt water, and concrete pore solution. In: American Society for Composites, 16th technical conference. Proceedings. September 9–12, 2001, Blacksburg, pp 1–12
34. Antheunis H et al (2010) Autocatalytic equation describing the change in molecular weight during hydrolytic degradation of aliphatic polyesters. Biomacromolecules 11(4):1118–1124
35. Ehrenfried LM, Farrar D, Cameron RE (2009) Degradation properties of co-continuous calcium-phosphate-polyester composites. Biomacromolecules 10(7):1976–1985
36. Zimmerman MC et al (1991) The design and analysis of laminated degradable composite bone plates for fracture fixation. In: High-Tech Fibrous Materials. American Chemical Society, Washington, DC, pp 132–148
37. Arnold C et al (2010) Design optimisation of carbon fibre epoxy composites operating in humid atmospheres. In: Composites UK—10th annual conference: innovation in composites 2010. Birmingham, UK
38. Bunsell AR, Renard J (2005) Fundamentals of fibre reinforced composite materials. IOP Publishing Ltd., UK
39. Litherland KL, Oakley DR, Proctor BA (1981) The use of accelerated ageing procedures to predict the long term strength of GRC composites. Cem Concr Res 11(3):455–466
40. Deng M et al (2008) A study on in vitro degradation behavior of a poly(glycolide-co-l-lactide) monofilament. Acta Biomater 4(5):1382–1391